Determination of the average lifetime of *b*-baryons

DELPHI Collaboration

P.Abreu[21], W.Adam[50], T.Adye[37], E.Agasi[31], I.Ajinenko[42], R.Aleksan[39], G.D.Alekseev[16], R.Alemany[49], P.P.Allport[22], S.Almehed[24], U.Amaldi[9], S.Amato[47], A.Andreazza[28], M.L.Andrieux[14], P.Antilogus[9], W-D.Apel[17], Y.Arnoud[39], B.Åsman[44], J-E.Augustin[19], A.Augustinus[9], P.Baillon[9], P.Bambade[19], F.Barao[21], R.Barate[14], M.Barbi[47], D.Y.Bardin[16], A.Baroncelli[40], O.Barring[24], J.A.Barrio[26], W.Bartl[50], M.J.Bates[37], M.Battaglia[15], M.Baubillier[23], J.Baudot[39], K-H.Becks[52], M.Begalli[6], P.Beilliere[8], Yu.Belokopytov[9,⋆], K.Belous[42], A.C.Benvenuti[5], M.Berggren[47], D.Bertrand[2], F.Bianchi[45], M.Bigi[45], M.S.Bilenky[16], P.Billoir[23], D.Bloch[10], M.Blume[52], S.Blyth[35], T.Bolognese[39], M.Bonesini[28], W.Bonivento[28], P.S.L.Booth[22], G.Borisov[42], C.Bosio[40], S.Bosworth[35], O.Botner[48], E.Boudinov[31], B.Bouquet[19], C.Bourdarios[9], T.J.V.Bowcock[22], M.Bozzo[13], P.Branchini[40], K.D.Brand[36], T.Brenke[52], R.A.Brenner[15], C.Bricman[2], L.Brillault[23], R.C.A.Brown[9], P.Bruckman[18], J-M.Brunet[8], L.Bugge[33], T.Buran[33], T.Burgsmueller[52], P.Buschmann[52], A.Buys[9], S.Cabrera[49], M.Caccia[28], M.Calvi[28], A.J.Camacho Rozas[41], T.Camporesi[9], V.Canale[38], M.Canepa[13], K.Cankocak[44], F.Cao[2], F.Carena[9], L.Carroll[22], C.Caso[13], M.V.Castillo Gimenez[49], A.Cattai[9], F.R.Cavallo[5], L.Cerrito[38], V.Chabaud[9], M.Chapkin[42], Ph.Charpentier[9], L.Chaussard[25], J.Chauveau[23], P.Checchia[36], G.A.Chelkov[16], M.Chen[2], R.Chierici[45], P.Chliapnikov[42], P.Chochula[7], V.Chorowicz[9], J.Chudoba[30], V.Cindro[43], P.Collins[9], J.L.Contreras[19], R.Contri[13], E.Cortina[49], G.Cosme[19], F.Cossutti[46], H.B.Crawley[1], D.Crennell[37], G.Crosetti[13], J.Cuevas Maestro[34], S.Czellar[15], E.Dahl-Jensen[29], J.Dahm[52], B.Dalmagne[19], M.Dam[29], G.Damgaard[29], P.D.Dauncey[37], M.Davenport[9], W.Da Silva[23], C.Defoix[8], A.Deghorain[2], G.Della Ricca[46], P.Delpierre[27], N.Demaria[35], A.De Angelis[9], W.De Boer[17], S.De Brabandere[2], C.De Clercq[2], C.De La Vaissiere[23], B.De Lotto[46], A.De Min[36], L.De Paula[47], C.De Saint-Jean[39], H.Dijkstra[9], L.Di Ciaccio[38], F.Djama[10], J.Dolbeau[8], M.Donszelmann[9], K.Doroba[51], M.Dracos[10], J.Drees[52], K.-A.Drees[52], M.Dris[32], Y.Dufour[9], D.Edsall[1], R.Ehret[17], G.Eigen[4], T.Ekelof[48], G.Ekspong[44], M.Elsing[52], J-P.Engel[10], N.Ershaidat[23], B.Erzen[43], E.Falk[24], D.Fassouliotis[32], M.Feindt[9], A.Ferrer[49], T.A.Filippas[32], A.Firestone[1], P.-A.Fischer[10], H.Foeth[9], E.Fokitis[32], F.Fontanelli[13], F.Formenti[9], B.Franek[37], P.Frenkiel[8], D.C.Fries[17], A.G.Frodesen[4], R.Fruhwirth[50], F.Fulda-Quenzer[19], J.Fuster[49], A.Galloni[22], D.Gamba[45], M.Gandelman[6], C.Garcia[49], J.Garcia[41], C.Gaspar[9], U.Gasparini[36], Ph.Gavillet[9], E.N.Gazis[32], D.Gele[10], J-P.Gerber[10], L.Gerdyukov[42], M.Gibbs[22], R.Gokieli[51], B.Golob[43], G.Gopal[37], L.Gorn[1], M.Gorski[51], Yu.Gouz[45,⋆], V.Gracco[13], E.Graziani[40], G.Grosdidier[19], K.Grzelak[51], S.Gumenyuk[28,⋆], P.Gunnarsson[44], M.Gunther[48], J.Guy[37], F.Hahn[9], S.Hahn[52], Z.Hajduk[18], A.Hallgren[48], K.Hamacher[52], W.Hao[31], F.J.Harris[35], V.Hedberg[24], R.Henriques[21], J.J.Hernandez[49], P.Herquet[2], H.Herr[9], T.L.Hessing[35], E.Higon[49], H.J.Hilke[9], T.S.Hill[1], S-O.Holmgren[44], P.J.Holt[35], D.Holthuizen[31], S.Hoorelbeke[2], M.Houlden[22], J.Hrubec[50], K.Huet[2], K.Hultqvist[44], J.N.Jackson[22], R.Jacobsson[44], P.Jalocha[18], R.Janik[7], Ch.Jarlskog[24], G.Jarlskog[24], P.Jarry[39], B.Jean-Marie[19], E.K.Johansson[44], L.Jonsson[24], P.Jonsson[24], C.Joram[9], P.Juillot[10], M.Kaiser[17], F.Kapusta[23], K.Karafasoulis[11], K.Karlsson[44], E.Karvelas[11], S.Katsanevas[3], E.C.Katsoufis[32], R.Keranen[4], Yu.Khokhlov[42], B.A.Khomenko[16], N.N.Khovanski[16], B.King[22], N.J.Kjaer[29], H.Klein[9], A.Klovning[4], P.Kluit[31], B.Koene[31], P.Kokkinias[11], M.Koratzinos[9], K.Korcyl[18], C.Kourkoumelis[3], O.Kouznetsov[13,16], P.-H.Kramer[52], M.Krammer[50], C.Kreuter[17], I.Kronkvist[24], Z.Krumstein[16], W.Krupinski[18], P.Kubinec[7], W.Kucewicz[18], K.Kurvinen[15], C.Lacasta[49], I.Laktineh[25], S.Lamblot[23], J.W.Lamsa[1], L.Lanceri[46], D.W.Lane[1], P.Langefeld[52], I.Last[22], J-P.Laugier[39], R.Lauhakangas[15], G.Leder[50], F.Ledroit[14], V.Lefebure[2], C.K.Legan[1], R.Leitner[30], Y.Lemoigne[39], J.Lemonne[2], G.Lenzen[52], V.Lepeltier[19], T.Lesiak[36], D.Liko[50], R.Lindner[52], A.Lipniacka[36], I.Lippi[36], B.Loerstad[24], J.G.Loken[35], J.M.Lopez[41], D.Loukas[11], P.Lutz[39], L.Lyons[35], J.MacNaughton[50], G.Maehlum[17], A.Maio[21], V.Malychev[16], F.Mandl[50], J.Marco[41], R.Marco[41], B.Marechal[47], M.Margoni[36], J-C.Marin[9], C.Mariotti[40], A.Markou[11], T.Maron[52], C.Martinez-Rivero[41], F.Martinez-Vidal[49], S.Marti i Garcia[49], J.Masik[30], F.Matorras[41], C.Matteuzzi[9], G.Matthiae[38], M.Mazzucato[36], M.Mc Cubbin[9], R.Mc Kay[1], R.Mc Nulty[22], J.Medbo[48], M.Merk[31], C.Meroni[28], S.Meyer[17], W.T.Meyer[1], M.Michelotto[36], E.Migliore[45], L.Mirabito[25], W.A.Mitaroff[50], U.Mjoernmark[24], T.Moa[44], R.Moeller[29], K.Moenig[9], M.R.Monge[13], P.Morettini[13], H.Mueller[17], L.M.Mundim[6], W.J.Murray[37], B.Muryn[18], G.Myatt[35], F.Naraghi[14], F.L.Navarria[5], S.Navas[49], K.Nawrocki[51], P.Negri[28], S.Nemecek[12], W.Neumann[52], N.Neumeister[50], R.Nicolaidou[3], B.S.Nielsen[29], M.Nieuwenhuizen[31], V.Nikolaenko[10], P.Niss[44], A.Nomerotski[36], A.Normand[35], W.Oberschulte-Beckmann[17], V.Obraztsov[42], A.G.Olshevski[16], A.Onofre[21], R.Orava[15], K.Osterberg[15], A.Ouraou[39], P.Paganini[19], M.Paganoni[9], P.Pages[10], H.Palka[18], Th.D.Papadopoulou[32], K.Papageorgiou[11], L.Pape[9], C.Parkes[35], F.Parodi[13], A.Passeri[40], M.Pegoraro[36], L.Peralta[21], H.Pernegger[50], A.Perrotta[5], C.Petridou[46], A.Petrolini[13], M.Petrovyck[28,⋆], H.T.Phillips[37], G.Piana[13], F.Pierre[39], M.Pimenta[21], M.Pindo[28], S.Plaszczynski[19], O.Podobrin[17], M.E.Pol[6], G.Polok[18], P.Poropat[46], V.Pozdniakov[16], M.Prest[46], P.Privitera[38], N.Pukhaeva[16], A.Pullia[28], D.Radojicic[35], S.Ragazzi[28], H.Rahmani[32], P.N.Ratoff[20], A.L.Read[33], M.Reale[52], P.Rebecchi[19], N.G.Redaelli[28], M.Regler[50], D.Reid[9], P.B.Renton[35], L.K.Resvanis[3], F.Richard[19], J.Richardson[22], J.Ridky[12], G.Rinaudo[45], I.Ripp[39], A.Romero[45], I.Roncagliolo[13], P.Ronchese[36], L.Roos[14], E.I.Rosenberg[1], E.Rosso[9], P.Roudeau[19], T.Rovelli[5], W.Ruckstuhl[31],

V.Ruhlmann-Kleider[39], A.Ruiz[41], K.Rybicki[18], H.Saarikko[15], Y.Sacquin[39], A.Sadovsky[16], G.Sajot[14], J.Salt[49], J.Sanchez[26], M.Sannino[13], M.Schimmelpfennig[17], H.Schneider[17], U.Schwickerath[17], M.A.E.Schyns[52], G.Sciolla[45], F.Scuri[46], P.Seager[20], Y.Sedykh[16], A.M.Segar[35], A.Seitz[17], R.Sekulin[37], R.C.Shellard[6], I.Siccama[31], P.Siegrist[39], S.Simonetti[39], F.Simonetto[36], A.N.Sisakian[16], B.Sitar[7], T.B.Skaali[33], G.Smadja[25], N.Smirnov[42], O.Smirnova[16], G.R.Smith[37], O.Solovianov[42], R.Sosnowski[51], D.Souza-Santos[6], T.Spassov[21], E.Spiriti[40], P.Sponholz[52], S.Squarcia[13], C.Stanescu[40], S.Stapnes[33], I.Stavitski[36], F.Stichelbaut[9], A.Stocchi[19], J.Strauss[50], R.Strub[10], B.Stugu[4], M.Szczekowski[51], M.Szeptycka[51], T.Tabarelli[28], J.P.Tavernet[23], O.Tchikilev[42], A.Tilquin[27], J.Timmermans[31], L.G.Tkatchev[16], T.Todorov[10], D.Z.Toet[31], A.Tomaradze[2], B.Tome[21], A.Tonazzo[28], L.Tortora[40], G.Transtromer[24], D.Treille[9], W.Trischuk[9], G.Tristram[8], A.Trombini[19], C.Troncon[28], A.Tsirou[9], M-L.Turluer[39], I.A.Tyapkin[16], M.Tyndel[37], S.Tzamarias[22], B.Ueberschaer[52], O.Ullaland[9], V.Uvarov[42], G.Valenti[5], E.Vallazza[9], C.Vander Velde[2], G.W.Van Apeldoorn[31], P.Van Dam[31], W.K.Van Doninck[2], J.Van Eldik[31], N.Vassilopoulos[35], G.Vegni[28], L.Ventura[36], W.Venus[37], F.Verbeure[2], M.Verlato[36], L.S.Vertogradov[16], D.Vilanova[39], P.Vincent[25], L.Vitale[46], E.Vlasov[42], A.S.Vodopyanov[16], V.Vrba[12], H.Wahlen[52], C.Walck[44], F.Waldner[46], M.Weierstall[52], P.Weilhammer[9], C.Weiser[17], A.M.Wetherell[9], D.Wicke[52], J.H.Wickens[2], M.Wielers[17], G.R.Wilkinson[35], W.S.C.Williams[35], M.Winter[10], M.Witek[18], K.Woschnagg[48], K.Yip[35], O.Yushchenko[42], F.Zach[25], A.Zaitsev[42], A.Zalewska[18], P.Zalewski[51], D.Zavrtanik[43], E.Zevgolatakos[11], N.I.Zimin[16], M.Zito[39], D.Zontar[43], R.Zuberi[35], G.C.Zucchelli[44], G.Zumerle[36]

[1] Ames Laboratory and Department of Physics, Iowa State University, Ames IA 50011, USA
[2] Physics Department, Univ. Instelling Antwerpen, Universiteitsplein 1, B-2610 Wilrijk, Belgium
 and IIHE, ULB-VUB, Pleinlaan 2, B-1050 Brussels, Belgium
 and Faculté des Sciences, Univ. de l'Etat Mons, Av. Maistriau 19, B-7000 Mons, Belgium
[3] Physics Laboratory, University of Athens, Solonos Str. 104, GR-10680 Athens, Greece
[4] Department of Physics, University of Bergen, Allégaten 55, N-5007 Bergen, Norway
[5] Dipartimento di Fisica, Università di Bologna and INFN, Via Irnerio 46, I-40126 Bologna, Italy
[6] Centro Brasileiro de Pesquisas Físicas, rua Xavier Sigaud 150, RJ-22290 Rio de Janeiro, Brazil
 and Depto. de Física, Pont. Univ. Católica, C.P. 38071 RJ-22453 Rio de Janeiro, Brazil
 and Inst. de Física, Univ. Estadual do Rio de Janeiro, rua São Francisco Xavier 524, Rio de Janeiro, Brazil
[7] Comenius University, Faculty of Mathematics and Physics, Mlynska Dolina, SK-84215 Bratislava, Slovakia
[8] Collège de France, Lab. de Physique Corpusculaire, IN2P3-CNRS, F-75231 Paris Cedex 05, France
[9] CERN, CH-1211 Geneva 23, Switzerland
[10] Centre de Recherche Nucléaire, IN2P3 - CNRS/ULP - BP20, F-67037 Strasbourg Cedex, France
[11] Institute of Nuclear Physics, N.C.S.R. Demokritos, P.O. Box 60228, GR-15310 Athens, Greece
[12] FZU, Inst. of Physics of the C.A.S. High Energy Physics Division, Na Slovance 2, 180 40, Praha 8, Czech Republic
[13] Dipartimento di Fisica, Università di Genova and INFN, Via Dodecaneso 33, I-16146 Genova, Italy
[14] Institut des Sciences Nucléaires, IN2P3-CNRS, Université de Grenoble 1, F-38026 Grenoble Cedex, France
[15] Research Institute for High Energy Physics, SEFT, P.O. Box 9, FIN-00014 Helsinki, Finland
[16] Joint Institute for Nuclear Research, Dubna, Head Post Office, P.O. Box 79, 101 000 Moscow, Russian Federation
[17] Institut für Experimentelle Kernphysik, Universität Karlsruhe, Postfach 6980, D-76128 Karlsruhe, Germany
[18] Institute of Nuclear Physics and University of Mining and Metalurgy, Ul. Kawiory 26a, PL-30055 Krakow, Poland
[19] Université de Paris-Sud, Lab. de l'Accélérateur Linéaire, IN2P3-CNRS, Bât. 200, F-91405 Orsay Cedex, France
[20] School of Physics and Materials, University of Lancaster, Lancaster LA1 4YB, UK
[21] LIP, IST, FCUL - Av. Elias Garcia, 14-1°, P-1000 Lisboa Codex, Portugal
[22] Department of Physics, University of Liverpool, P.O. Box 147, Liverpool L69 3BX, UK
[23] LPNHE, IN2P3-CNRS, Universités Paris VI et VII, Tour 33 (RdC), 4 place Jussieu, F-75252 Paris Cedex 05, France
[24] Department of Physics, University of Lund, Sölvegatan 14, S-22363 Lund, Sweden
[25] Université Claude Bernard de Lyon, IPNL, IN2P3-CNRS, F-69622 Villeurbanne Cedex, France
[26] Universidad Complutense, Avda. Complutense s/n, E-28040 Madrid, Spain
[27] Univ. d'Aix - Marseille II - CPP, IN2P3-CNRS, F-13288 Marseille Cedex 09, France
[28] Dipartimento di Fisica, Università di Milano and INFN, Via Celoria 16, I-20133 Milan, Italy
[29] Niels Bohr Institute, Blegdamsvej 17, DK-2100 Copenhagen 0, Denmark
[30] NC, Nuclear Centre of MFF, Charles University, Areal MFF, V Holesovickach 2, 180 00, Praha 8, Czech Republic
[31] NIKHEF-H, Postbus 41882, NL-1009 DB Amsterdam, The Netherlands
[32] National Technical University, Physics Department, Zografou Campus, GR-15773 Athens, Greece
[33] Physics Department, University of Oslo, Blindern, N-1000 Oslo 3, Norway
[34] Dpto. Fisica, Univ. Oviedo, C/P. Pérez Casas, S/N-33006 Oviedo, Spain
[35] Department of Physics, University of Oxford, Keble Road, Oxford OX1 3RH, UK
[36] Dipartimento di Fisica, Università di Padova and INFN, Via Marzolo 8, I-35131 Padua, Italy
[37] Rutherford Appleton Laboratory, Chilton, Didcot OX11 OQX, UK
[38] Dipartimento di Fisica, Università di Roma II and INFN, Tor Vergata, I-00173 Rome, Italy
[39] Centre d'Etudes de Saclay, DSM/DAPNIA, F-91191 Gif-sur-Yvette Cedex, France
[40] Istituto Superiore di Sanità, Ist. Naz. di Fisica Nucl. (INFN), Viale Regina Elena 299, I-00161 Rome, Italy
[41] Instituto de Fisica de Cantabria (CSIC-UC), Avda. los Castros, S/N-39006 Santander, Spain, (CICYT-AEN93-0832)
[42] Inst. for High Energy Physics, Serpukov P.O. Box 35, Protvino, (Moscow Region), Russian Federation
[43] J. Stefan Institute and Department of Physics, University of Ljubljana, Jamova 39, SI-61000 Ljubljana, Slovenia
[44] Fysikum, Stockholm University, Box 6730, S-113 85 Stockholm, Sweden
[45] Dipartimento di Fisica Sperimentale, Università di Torino and INFN, Via P. Giuria 1, I-10125 Turin, Italy
[46] Dipartimento di Fisica, Università di Trieste and INFN, Via A. Valerio 2, I-34127 Trieste, Italy
 and Istituto di Fisica, Università di Udine, I-33100 Udine, Italy
[47] Univ. Federal do Rio de Janeiro, C.P. 68528 Cidade Univ., Ilha do Fundão BR-21945-970 Rio de Janeiro, Brazil

[48] Department of Radiation Sciences, University of Uppsala, P.O. Box 535, S-751 21 Uppsala, Sweden
[49] IFIC, Valencia-CSIC, and D.F.A.M.N., U. de Valencia, Avda. Dr. Moliner 50, E-46100 Burjassot (Valencia), Spain
[50] Institut für Hochenergiephysik, Österr. Akad. d. Wissensch., Nikolsdorfergasse 18, A-1050 Vienna, Austria
[51] Inst. Nuclear Studies and University of Warsaw, Ul. Hoza 69, PL-00681 Warsaw, Poland
[52] Fachbereich Physik, University of Wuppertal, Postfach 100 127, D-42097 Wuppertal, Germany

[*] On leave of absence from IHEP Serpukhov

Abstract. The average lifetime of b-baryons has been studied using 3×10^6 hadronic Z^0 decays collected by the DELPHI detector at LEP. Three methods have been used, based on the measurement of different observables: the proper decay time distribution of 206 vertices reconstructed with a Λ, a lepton and an oppositely charged pion; the impact parameter distribution of 441 muons with high transverse momentum accompanied by a Λ in the same jet; and the proper decay time distribution of 125 Λ_c-lepton decay vertices with the Λ_c exclusively reconstructed through its $pK\pi$, pK^0 and $\Lambda 3\pi$ decay modes. The combined result is:

$$\tau(b\text{-baryon}) = (1.254\,^{+0.121}_{-0.109}(stat)$$
$$\pm 0.04(syst)\,^{+0.03}_{-0.05}(syst))\ \text{ps}$$

where the first systematic error is due to experimental uncertainties and the second to the uncertainties in the modelling of the b-baryon production and semi-leptonic decay. Including the measurement recently published by DELPHI based on a sample of proton-muon vertices, the average b-baryon lifetime is :

$$\tau(b\text{-baryon}) = (1.255\,^{+0.115}_{-0.102}(stat)\ \pm 0.05)\ ps.$$

1 Introduction

Baryons containing a beauty quark, referred to as b-baryons throughout this paper, were first observed by the UA1 and SFM experiments, which reported signals for the exclusive Λ_b decays into $J/\psi\Lambda$ [1] and $pD^0\pi^-$ and $\Lambda_c^+\pi^-\pi^+\pi^-$ [2] respectively. At LEP, evidence for b-baryon production in Z^0 hadronic decays was found [3, 4] in the correlation observed between Λ's or Λ_c's and leptons (ℓ's). Using this correlation, first measurements of the average b-baryon lifetime were made [4, 5]. It is predicted to be shorter than that of B mesons, but only by some $(5 - 10)\%$ [6]. But current experimental data [7, 8] indicate a substantially shorter lifetime that would be difficult to accommodate theoretically. It is therefore important to pursue these measurements further.

This paper updates the recent DELPHI results on the average lifetime of b-baryons based on the proper time distribution of partially reconstructed b-baryon decay candidates containing a Λ or a Λ_c correlated with a lepton [8]. The $\Lambda_c \to pK^o$ and $\Lambda_c \to \Lambda 3\pi$ decay modes are added to the $\Lambda_c \to pK\pi$ mode previously used in the exclusive reconstruction of Λ_c particles, an analysis based on the the impact parameter distribution of muons in the same jet as a Λ is also added, and the data collected in 1994 are included.

2 The DELPHI detector

The DELPHI detector and its performance have been described in detail elsewhere [9, 10]. Both the charged particle tracking through the uniform axial field and the particle identification are important in this analysis. The detector elements used for tracking are the Vertex Detector (VD), the Inner Detector (ID), the Time Projection Chamber (TPC) and the Outer Detector (OD). The VD provides the high precision needed near the primary vertex. Hadron identification is based mainly on the Ring Imaging Cherenkov detector (RICH), and lepton identification on the barrel electromagnetic calorimeter (HPC) and the muon chambers; supplementary information is provided by the ionisation loss measurements in the TPC.

For the data taken from 1991 to 1993, the VD consisted of 3 cylindrical layers of silicon detectors (radii 6.3, 9.0 and 10.9 cm) measuring points in the plane transverse to the beam direction ($r\phi$ coordinate) in the polar angle range $43° < \theta < 137°$. In 1994, two layers were equipped with detector modules with double sided readout providing a single hit precision of 7.6 μm in the $r\phi$ coordinate, similar to that obtained previously, and 9 μm in the coordinate parallel to the beam (z) [11]. For high momentum tracks with associated hits in the VD, the extrapolation precision close to the interaction region was 20 μm in the $r\phi$ plane and 34 μm in the rz plane.

Charged particle tracks were reconstructed with 95% efficiency and with a momentum resolution $\sigma_p/p < 2.0 \times 10^{-3}p$ (GeV/c) in the polar angle region $25° < \theta < 155°$. The primary vertex of the e^+e^- interaction was reconstructed on an event-by-event basis using a beam spot constraint. The position of the primary vertex could be determined in this way [10] to a precision of about 40μm (slightly dependent on the flavour of the primary quark-antiquark pair) in the plane transverse to the beam direction. In this plane, secondary vertices from beauty and charm decays were reconstructed with a precision of about 300 μm along the flight direction of the decaying particle.

The RICH detector [12] consisted of two parts. A liquid radiator provided $p/K/\pi$ separation in the momentum range 2.5–8 GeV/c by measuring the size of the Cherenkov angle with an average precision of 13 mrad, corresponding for example to 3% for a proton with a momentum of 3 GeV/c. A gas radiator separated protons from kaons between 16 and 30 GeV/c in the same way, and also provided proton selection in the intermediate 8–16 GeV/c momentum range, where protons gave no Cherenkov light, by vetoing pions and kaons. The dE/dx measurement had a precision of $\pm 7\%$ in the momentum range $4 < p < 25$ GeV/c.

The barrel electromagnetic calorimeter (HPC) covered the polar angle region $46° < \theta < 134°$ and detected electrons with an energy precision $\sigma_E/E = 0.04 \oplus 0.33/\sqrt{E}$ (E in GeV). Two layers of muon chambers covered the polar angle region $20° < \theta < 160°$, except for two regions of $\pm 3°$ around $\theta = 42°$ and $\theta = 138°$. The first layer consisted of three planes of chambers and was inside the return yoke of the magnet, after 90 cm of iron, while the second, with two chamber planes, was mounted outside the yoke, behind a further 20 cm of iron.

3 Hadronic Z^0 selection and particle identification

Hadronic events from Z^0 decays were selected by requiring a charged multiplicity greater than 4 and a total reconstructed energy greater than $0.12\sqrt{s}$, where $\sqrt{s}$ is the centre of mass energy; charged particles were required to have a momentum greater than 0.4 GeV/c and a polar angle between $20°$ and $160°$. The overall trigger and selection efficiency was 0.9500 ± 0.0011 [13]. An identified lepton was required in the event; only tracks with momentum bigger than 3 GeV/c were considered as possible lepton candidates.

Lepton identification in the DELPHI detector is described in [10]. The probability of a track being an electron was calculated using a) the spatial separation between its extrapolated position at the HPC and the position of the nearest electromagnetic shower, b) a comparison between its momentum and the measured energy, and c) a successful fit to the longitudinal profile of the shower in the 9 HPC layers. The dE/dx measurement in the TPC was used in the algorithm as independent and complementary information. With the selections applied, the electron identification efficiency inside the angular acceptance of the HPC was found to be $(65\pm1)\%$ and the hadron misidentification probability 0.4%.

The probability of a track being a muon was calculated from a global χ^2 of the match between its extrapolation to the muon chambers and the hits observed there. With the selections applied, the muon identification efficiency was $(86\pm1)\%$ and the hadron misidentification probability $(0.7\pm0.1)\%$.

Hadron identification in the DELPHI detector is also described in [10]. The analysis presented in this paper used protons in a momentum range well above the pion threshold in the gas radiator of 2.5 GeV/c. Above this threshold, the gas radiator vetoed pions up to 16 GeV/c. The average proton selection efficiency was 75% (varying slightly with the momentum) for a pion rejection factor of 15. Kaons were vetoed in the same way between 8.5 GeV/c, the gas radiator threshold for kaons, and 16 GeV/c. Above 16 GeV/c, identification was provided by the measurement of the Cherenkov angle of the detected photons [10, 14], with $(80 \pm 10)\%$ efficiency and rejection factors of 5-10. The algorithms were also applied to the liquid radiator data, which provided complementary information for K/π and K/p separation in the momentum range 1-7 GeV/c.

The DELPHI simulation program [10] included full simulation of the detector response. It used the JETSET Parton Shower event generator [15], with a b-baryon production rate reproducing the experimentally observed rate [8]. In the simulation, the generated lifetime of all weakly decaying b-
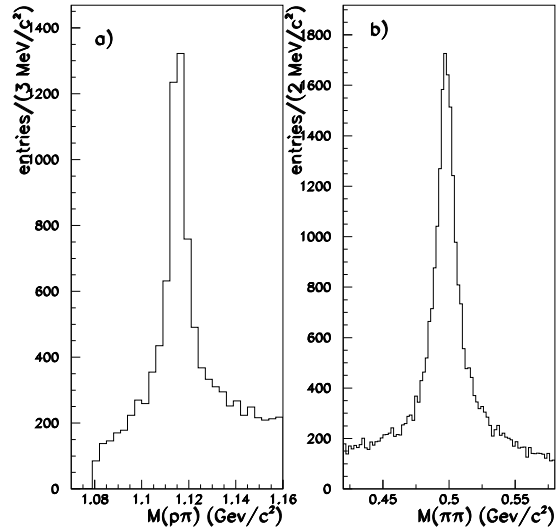

Fig. 1. a) $p\pi$ and **b)** $\pi\pi$ invariant mass distributions for oppositely charged pairs of particles, selected as two-prong decay candidates, having a momentum sum greater than 4 GeV/c and accompanied by a lepton of momentum greater than 3 GeV/c in the same hemisphere

baryons was 1.3 ps. About 5 million simulated Z^0 hadronic decays were used in the analysis.

4 Λ and K^0 reconstruction

Λ particles were used in the Λ-lepton analyses and in the reconstruction of the $\Lambda_c \to \Lambda 3\pi$ decay mode in the Λ_c-lepton analysis. K^0 mesons were used to reconstruct the $\Lambda_c \to pK^0$ decays.

The $\Lambda \to p\pi$ and $K^0 \to \pi\pi$ decays were reconstructed if the distance in the $r\phi$ plane between the Λ decay point and primary vertex was less than 90cm. This condition meant that the decay products had track segments at least 20cm long in the TPC. The reconstruction of two-prong decays in the DELPHI detector is described in detail in [10]. In addition to the selection criteria defined there, the Λ selection required a loose particle identification for the decay product of higher momentum, assumed to be the proton: the Λ candidate was retained if the proton candidate had a measured dE/dx at least one standard deviation below the value expected for the pion hypothesis or was tagged as a proton by the RICH. For Λ particles with a momentum above 4 GeV/c, this requirement reduced the combinatorial background by about a factor of two, with negligible efficiency loss. The efficiencies for the decay modes considered varied between 35% and 10% in the Λ/K^0 momentum range 2-20 GeV/c.

The invariant mass plots for accepted Λ and K^0 candidates with $p > 4$ GeV/c accompanied by a lepton with $p > 3$ GeV/c in the same hemisphere (defined by the thrust axis) are shown in Figs. 1a,b respectively.

5 Lifetime measurements using $\Lambda\ell$ pairs

Decays of b-baryons giving a Λ-lepton ($\Lambda\ell$) pair in the final state are thought to originate mainly from b-baryon decays

into $\Lambda_c \ell \nu X$ with $\Lambda_c \to \Lambda X'$, where X and X' are any particles. Typically, the lepton has high transverse momentum, p_T, with respect to the jet direction, defined below, and also high longitudinal momentum. Also, the Λ has a harder momentum spectrum than the Λ's produced in light quark fragmentation. In the following, the selection of the $\Lambda \ell$ pairs required the momentum of the Λ candidate to be greater than 4 GeV/c and the momentum of the lepton to be greater than 3 GeV/c.

Background sources of $\Lambda \ell$ in the same jet were:
- B meson semileptonic decays such as $B \to \Lambda_c \bar{N} \ell^- \nu X$ (where $\bar{N}$ is an antibaryon),
- Λ_c semileptonic decays
- accidental correlations of a Λ candidate and a lepton.

In both b-baryon and B meson decays, the proton from the Λ decay has the opposite sign to the lepton, i.e. the pairs are $p\ell^-$ not $p\ell^+$ (charged conjugate states are always implied throughout this paper). This combination is referred to as *right sign*. However, the contribution of semileptonic B meson decays has been estimated to be negligible [8].

Background events from direct c production through the $c \to \Lambda_c \to \Lambda \ell \nu X$ decay chain have protons and leptons of the same sign (referred to as *wrong sign* combinations in the following); but the lepton p_T spectrum is softer, so this background was reduced to a negligible amount by the p_T and $\Lambda \ell$ invariant mass cuts defined below.

Two methods using $\Lambda \ell$ pairs were developed for the determination of the average b-baryon lifetime. The first one was based on the reconstruction of b-baryon candidate decay vertices using the Λ, the lepton (e or μ) and an additional track supposed to come from the b-baryon decay chain. The proper time distribution of these candidate vertices was fitted. The second method used only the events with a Λ and a muon and was based on the impact parameter distribution of the muons.

5.1 The proper time distribution analysis

In this analysis, the b-baryon decay chain was partially reconstructed using a Λ, a lepton in the same jet as the Λ, and an oppositely charged track selected by the procedure described below. Charged and neutral particles were clustered into jets using the LUND jet finding algorithm LUCLUS [16] with a clustering mass parameter equal to 2.5 GeV/c^2.

The lepton was accepted if its p_T, computed including the lepton in the jet (p_T^{in}), was greater than 0.6 GeV/c. The $\Lambda \ell$ pair was required to have an invariant mass in the range 2.0 to 4.5 GeV/c^2 and a total momentum greater than 9 GeV/c.

The determination of the average b-baryon lifetime was based on the reconstruction of the decay vertex and hence the decay length with respect to the reconstructed primary vertex [10]. Since the extrapolation of the Λ flight direction to the interaction region was not precise enough to separate secondary from tertiary vertices in the b-baryon decay chain, a unique secondary vertex was reconstructed using the Λ, the correlated high p_T lepton and an oppositely charged particle (assumed to be a pion) with momentum greater than 0.5 GeV/c. The χ^2 probability of the vertex fit was required to be greater than 0.001. The lepton and the candidate pion
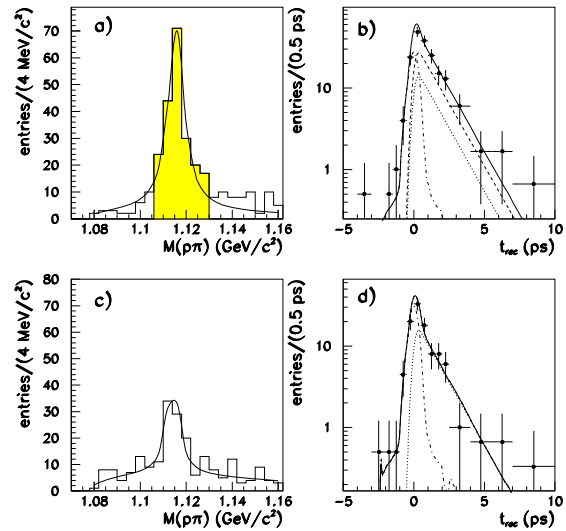

Fig. 2. Λ candidate mass distributions for reconstructed $\Lambda \ell \pi$ vertices of **a)** right sign and **c)** wrong sign respectively. **b)** The lifetime distribution for 206 b-baryon candidates, i.e. right sign $\Lambda \ell \pi$ vertices with $1.106 < M(p\pi) < 1.130$ GeV/c^2 (shaded area in the Λ mass plot); **d)** The lifetime distribution of the background sample defined in the text. The full lines represent the result of the fits described in the text; in **b)** and **d)** the dashed line is the estimated b-baryon contribution and the dotted and dot-dashed lines represent the flying and non-flying backgrounds respectively

were each required to have at least two associated hits in the vertex detector. To reduce the combinatorial background, the ($\Lambda \ell \pi$) invariant mass had to be less than 5.8 GeV/c^2 and the ($\Lambda \pi$) invariant mass less than 2.3 GeV/c^2. If more than one pion gave a vertex which passed the above cuts, the highest momentum one was chosen. In the simulation, in 90% of the cases the candidate pion associated to the vertex did originate from the Λ_b decay chain. Out of 532 (280) right sign (wrong sign) $\Lambda \ell$ events with $1.106 < M(p\pi) < 1.130$ GeV/c^2, 206 (113) decay vertices were reconstructed. The corresponding ($p\pi$) invariant mass plots are shown in Figs. 2a,c respectively.

The b-baryon purity of the sample after the vertex reconstruction, F_s, was determined from the data by a fit to the mass plots for the right and wrong sign correlations (Figs. 2a,c). In the simulation, the background from a true Λ accidentally accompanied by a lepton was found to be $(8 \pm 3)\%$ bigger in the wrong sign sample than in the right sign sample. This asymmetry was due to the contribution from events with both a b-baryon and a $\bar{\Lambda}$ from the primary interaction in the same jet, in which the b-baryon decayed semileptonically and the $\bar{\Lambda}$ was reconstructed. Taking into account this difference and assuming the number of background events from all the other sources of accidental combinations to be the same in both samples, as predicted by the simulation, the b-baryon purity of the signal sample was found to be $F_s = (55 \pm 5)\%$.

After the selection described above, background events were dominated by accidental combinations of a Λ candidate (either a true Λ from the primary vertex or a fake Λ) and a lepton candidate (mostly true leptons). They contained fake vertices constructed using charged tracks from the primary vertex only, and also vertices using tracks originating
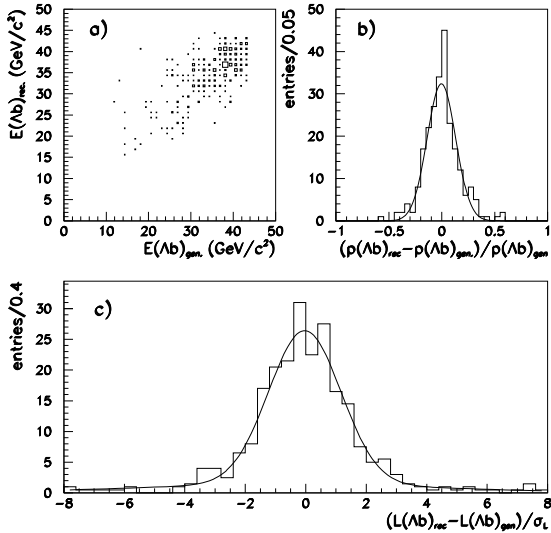
Fig. 3. a) Reconstructed vs generated b-baryon energy and **b)** distribution of the difference between reconstructed and generated momentum, normalised to the generated momentum, in the simulation sample; **c)** pull distribution for the reconstructed position of the b-baryon in the plane transverse to the beam direction. The curves in **b)** and **c)** represent the results of a Gaussian and a double Gaussian fit respectively to the distributions

from charm and B meson decays. The time distribution of the former component (the *"non-flying background"*) was parametrised by two Gaussian functions centred on zero with widths determined by the detector resolution. The fraction of the total background, F_{fb}, due to the latter component (the *"flying background"*) and its average lifetime were determined from the data by the fitting procedure described below. The fraction of the background due to the non-flying component, F_{nf}, was then determined by the normalisation equation: $F_{fb} + F_{nf} = 1$.

The b-baryon momentum was estimated using the *residual energy* technique. The residual energy, E_{res}, was computed by subtracting the energies of the Λ, E_Λ, the lepton, E_ℓ, and the pion, E_π, from the total "visible" energy, E_{vis}, in the hemisphere, defined by the plane perpendicular to the total momentum p_{tot} of those three particles, that contained the Λ and the lepton. The visible energy was defined as the sum of the energies of the charged particles, assumed to be pions, and of the electromagnetic shower energies not associated to charged tracks. The energy of the b-baryon, E_{Λ_b}, was then estimated from the equation:

$$E_{\Lambda_b} = E_{beam} - E_{res} = E_{beam} - E_{vis} + E_\Lambda + E_\ell + E_\pi$$

where E_{beam} is the beam energy. This method of estimating the b-baryon energy assumes that all the unobserved energy is due to particles from the b-baryon decay and that all the residual energy is due to particles not from the b-baryon; this holds for the decay b-baryon $\to \Lambda \ell \nu \pi$ if only the energy of the neutrino is undetected. In the simulation an additional small correction (a factor 0.97 for unpolarised b-baryons) is needed to reproduce the generated spectrum [8]. This correction factor was therefore applied to the above value of E_i. The momentum p_{Λ_b} of the b-baryon was then deduced.

The correlation between the reconstructed and generated b-baryon energy and the resolution of the b-baryon

momentum are shown in Figs. 3a,b for a sample of simulated b-baryon $\to \Lambda_c l \nu$ decays. A Gaussian fit to the distribution in Fig. 3b gave a fractional b-baryon momentum error $\sigma_p/p = 0.14$; if additional pions were generated in the b-baryon semileptonic decay the resolution deteriorated to 18% and the correction factor increased. This effect was taken into account in the systematic errors, as discussed below.

A maximum likelihood fit was performed simultaneously to the lifetime distribution of the 206 events of the signal sample and to the 113 background vertices with the wrong sign which survived the same selection procedure as that used for the signal. The likelihood function f was defined as the sum of two exponential functions representing the time distributions of the signal and the flying background, each convoluted with a Gaussian function representing the experimental resolution, and a double Gaussian term representing the behaviour of the non-flying background. Thus the function to be maximised was

$$L = \Sigma_i \ln[f(t_i, \sigma_i, \tau, \tau_{bck}, F_{fb})],$$

with

$$f(t_i, \sigma_i, \tau, \tau_{bck}, F_{fb}) = F_s \cdot E(\tau) \otimes G(\sigma_i)$$

$$+(1 - F_s) \cdot [F_{fb} \cdot E(\tau_{bck}) \otimes G(\sigma_i)$$

$$+(1 - F_{fb}) \cdot ((1 - \gamma) \cdot G(\sigma_i) + \gamma \cdot G(k\sigma_i))]$$

where $E(x) = \frac{1}{x}\exp(-t_i/x)$ is a decreasing exponential with average x; τ and τ_{bck} are the signal and background lifetimes; and $G(\sigma_i)$ represents a Gaussian resolution function with standard deviation σ_i where σ_i is the error on the proper decay time t_i. The constants γ and k described the size and width of the second Gaussian describing the tail in the detector resolution distribution. They were fixed to the values 0.06 and 4.7 respectively, obtained in the simulation from a double Gaussian fit to the pull distribution for the reconstructed position of the b-baryon vertex shown in Fig. 3c. The decay time t_i was computed from the formula $t_i = (l_i/\sin\theta_i)/(p_i/M_{bar})$, where l_i is the measured decay length in the plane transverse to the beam direction, θ_i is the polar angle of the total momentum vector p_{tot}, p_i is the b-baryon momentum p_{Λ_b} estimated by the residual energy technique described above, and M_{bar} is the assumed b-baryon mass. The systematic error associated with the σ_i computation and the parametrisation of the non-flying background will be discussed below. The normalisation constant F_s for the signal fraction was fixed to the fitted value of the b-baryon purity discussed above in the right sign sample and was defined to be zero in the wrong sign sample. A three parameter fit to the data gave

$$\tau(b\text{-baryon})= 1.46^{+0.22}_{-0.21} \text{ ps}$$

with a background lifetime $\tau_{bck} = 1.37^{+0.21}_{-0.18}$ ps and $F_{fb} = 0.57 \pm 0.05$. The result of the fit for the lifetime was stable within 0.03 ps when changing the p_T cut on the lepton from 0.6 to 1.0 GeV/c (thus increasing the b-baryon purity of the sample from 0.55 to 0.62) and within 0.09 ps when changing the minimum accepted b-baryon energy from 15 to 40 GeV/c^2. The lifetime distributions for the signal events

Table 1. Correlation matrix between the variables of the lifetime fit to the proper flight time distribution of $\Lambda\ell\pi$ vertices

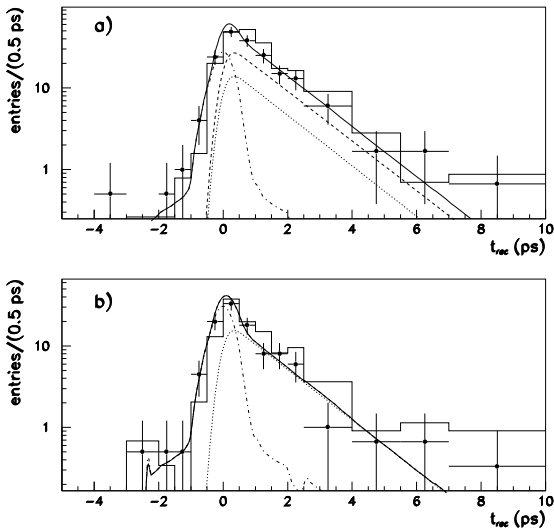| –	τ	$\tau_{\rm bck}$	$F_{\rm fb}$
τ	1.00		
$\tau_{\rm bck}$	−0.46	1.00	
$F_{\rm fb}$	−0.02	−0.25	1.00

Fig. 4. a) The lifetime distribution for b-baryon candidates obtained from $\Lambda\ell\pi$ vertices in real data (points with errors) compared with the signal sample from simulation (histogram). **b)** The same for the background sample. In the simulation, the generated b-baryon lifetime was 1.6 ps. The curves are as in Figs. 2b,d

and for the background, together with the probability functions resulting from the fit, are shown in Figs. 2b,d. The correlation matrix is shown in Table 1, where the anticorrelation between the signal and background lifetimes is quantified.

Figures 4a and 4b compare the distributions of the reconstructed lifetime in the data with the corresponding distributions in the simulation, obtained by applying the same reconstruction and selection procedure as in the data. The parts of the distributions for negative reconstructed flight time, which are sensitive to the behaviour of the detector resolution which was fixed from the simulation in the likelihood fit, show good agreement between real and simulated data.

To check the consistency of the method, the same analysis and fitting procedure was applied to the simulated event sample, containing about 200 reconstructed b-baryon decays generated with a lifetime of 1.3 ps. The result was $\tau(b$-baryon)$= 1.36 \pm 0.12$ ps and $\tau_{bck} = 1.54 \pm 0.13$ ps, with a b-baryon purity $F_s = (61 \pm 5)\%$ and a fitted flying background fraction $F_{fb} = 0.76 \pm 0.03$. This fraction correctly reproduced within the statistical error the fraction (0.75) of reconstructed decays in the simulated background sample in which at least one track originated from a weakly decaying particle.

The different contributions to the systematic uncertainty are listed in Table 2. The first one reflects the uncertainty in the signal purity, which was estimated from the fits to the right and wrong sign Λ mass peaks to be 0.55 ± 0.05. The

second one comes from the estimation of the error σ_i on the individual time measurements discussed below. The third is due to the possible bias introduced by the fit procedure. The remaining contributions affect the estimation of the b-baryon momentum.

The error σ_i was assumed to be Gaussian and estimated as :

$$\sigma_i = t_i \cdot \sqrt{(\sigma_l^i/l_i)^2 + (\sigma_p/p)^2 + (\sigma_{\sin\theta/\sin\theta})^2}$$

where σ_l^i is the error on the decay length l_i, and $\sigma_p/p = 0.14$ and $\sigma_{\sin\theta/\sin\theta} = 0.025$ are the resolutions on the estimated b-baryon momentum and direction found in the simulation. The error on the secondary vertex position in the simulation resulting from the vertex fit had to be scaled by a factor 1.5 to reproduce the observed spread of the difference between the reconstructed and generated decay lengths, as determined from the pull distribution of Fig. 3c. An uncertainty of ± 0.5 was conservatively assumed on the value of this rescaling factor, which was also used in the real data, leading to a contribution to the systematic error of ± 0.03 ps. Varying the resolution on the b-baryon momentum in the range $(14 - 18)\%$ to take into account the effect on σ_p/p of additional hadrons (other than the Λ_c) in the b-baryon semi-leptonic decay, changed the fit result by -0.02 ps. Finally, varying the constant γ describing the second Gaussian component of the non-flying background in the range $0 - 0.10$ changed the fitted b-baryon lifetime by ± 0.005 ps. Thus an overall contribution to the total systematic error of $^{+0.03}_{-0.04}$ ps was conservatively associated to the σ_i estimation.

To control the possible bias introduced by the fitting procedure, a fit to about 600 reconstructed b-baryon decays from a dedicated simulation sample of 30000 $\Lambda_b \rightarrow \Lambda_c l\nu$ decays generated with a lifetime of 1.30 ps gave $\tau(b$-baryon)$= 1.28 \pm 0.05$ ps. The statistical error of this result was considered as a systematic error from this possible error source.

The effect of the Λ_c decay mode uncertainty was computed in the simulation by varying within their experimental errors the relative amounts of the $\Lambda_c \rightarrow \Lambda\pi$, $\Lambda_c \rightarrow \Lambda\pi\pi^o$ and $\Lambda_c \rightarrow \Lambda 3\pi$ branching fractions [17]. The average value of the b-baryon energy, $< E_{\Lambda_b} >$, resulting from the fragmentation of the b-quark was assumed to be the same as the average value measured for b hadrons [18], with an uncertainty increased by a factor of 3 to take into account possible differences between b-baryon and B-meson fragmentation. Varying it by the quoted uncertainty changed the correction factor in the b-baryon momentum estimation by $\pm 0.7\%$. The assumed value of the average b-baryon mass, M_{bar}, was shifted by 30 MeV/c^2 with respect to the measured mass of the Λ_b , $M(\Lambda_b) = 5640 \pm 50$ MeV/c^2[1], to take into account the contribution of Ξ_b production (measured to be 5 times smaller than Λ_b production [19]), as the Ξ_b mass is expected to be 250 ± 50 MeV/c^2 higher than the Λ_b mass. The b-baryon semileptonic decay was simulated in the framework of Heavy Quark Effective Theory, using the Isgur-Wise function $\eta(\omega) = \exp[a_{IW}(1 - \omega)]$[20], where $\omega = v_{\Lambda_b} \cdot v_{\Lambda_c}$ and v_{Λ_b} (v_{Λ_c}) is the b-baryon (c-baryon) 4-velocity. The Λ_b polarisation systematic was evaluated following the recommendations of [21]. If resonant and non-resonant $\Lambda_b \rightarrow \Lambda_c\ell\nu + n\pi$ decays are an important fraction

Table 2. Contributions to the systematic error on the average b-baryon lifetime measured using the proper time distribution of $\Lambda\ell\pi$ vertices: the modelling uncertainties in the lower part of the table are fully correlated with corresponding errors in other analyses

Error source	Range of Variation	Syst. error (ps)
Signal Fraction F_s	0.55 ± 0.05	± 0.01
σ_i Parametrisation	see text	$^{+0.03}_{-0.04}$
Fit procedure bias	see text	± 0.05
Λ_c Decay Mode Uncertainty	one st. dev. [17]	± 0.02
$< E_{\Lambda_b} > /E_{beam}$	0.70 ± 0.03	± 0.01
M_{bar}	5670 ± 70 MeV	± 0.015
$\eta(\omega) = \exp[a_{IW}(1 - \omega)]$	$a_{IW} = 1.7^{+3.3}_{-1.7}$	± 0.01
Λ_b polarisation	-0.47 ± 0.47	± 0.01
$Br(\Lambda_b \to \Lambda_c \ell\nu n\pi)/Br(\Lambda_b \to \Lambda_c \ell\nu)$	$0 \to 0.3$	-0.06
Total systematic error	—	$^{+0.07}_{-0.09}$

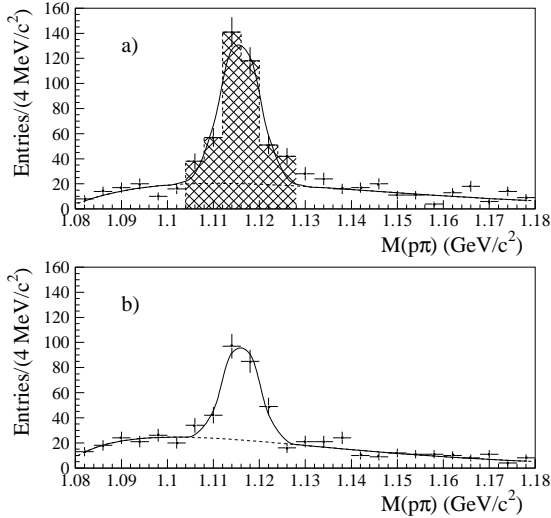**Fig. 5.** Λ candidate mass distributions for reconstructed $\Lambda\mu$ events of **a)** right sign and **b)** wrong sign respectively. The hatched region shows the events used in the impact parameter lifetime analysis

of the total decay width, where n is a positive integer, the b-baryon momentum estimation by the residual energy method must be further corrected. If the Λ_b semi-leptonic decay was assumed to be a 4 or 5 body decay in 30% of the cases, the fitted lifetime was shifted by -0.06 ps with respect to the value obtained for the $\Lambda_b \to \Lambda_c \ell\nu$ decay mode.

Summing the systematic uncertainties listed in Table 2 in quadrature gives an overall systematic uncertainty of $^{+0.07}_{-0.09}$ ps .

5.2 The muon impact parameter distribution analysis

In this analysis, only a Λ and a muon were reconstructed and the b-baryon lifetime was measured from the impact parameter distribution of the muons. Electron candidates were not used as bremsstrahlung radiation resulting from their passage through the detector material gave larger uncertainties in their impact parameters.

The muon candidates used were required to have at least two associated hits in the vertex detector, a momentum between 3 and 30 GeV/c, and a transverse momentum (p_T^{in}), defined as in the analysis described above, between 1 and

4 GeV/c. The Λ was required only to have a momentum above 4 GeV/c and a direction within $45°$ of the muon. The distributions of the Λ mass for the right sign and wrong sign $\Lambda\mu$ candidates are shown in Figs. 5a,b. To be used in the lifetime analysis, the Λ mass was required to lie between 1.104 and 1.128 GeV/c^2. A fit to the mass peak and background, as shown in the figure, gave the number of right sign events above background as 308 ± 21 out of a total of 441 events. The wrong sign sample gave 186 ± 19 out of 323 events. Correcting for the $(8 \pm 3)\%$ asymmetry in the background combinations described previously, and for a contribution of similar size where the muon is from charm decay, the b-baryon signal in the right sign sample was estimated to be 169 ± 30 events. This error estimate includes a contribution from varying the parametrisation used in the mass fit. This corresponds to a signal fraction, F_s, of 0.38 ± 0.07.

The lifetime of the b-baryons was estimated from the impact parameter distribution of the muon candidates satisfying the above requirements. The impact parameters, δ, of the muons were calculated relative to an average beamspot, determined from several hundred events recorded close in time to the b-baryon candidate event. The impact parameters were assigned a "lifetime-sign" [10], determined by whether the track crosses its associated jet axis in front of (positive sign) or behind (negative sign) the beamspot. Particles resulting from the decay of a b-baryon with a flight path along the jet axis would be expected to have only positive lifetime-signed impact parameters, in the absence of resolution effects.

The contribution of the b-baryon to the muon impact parameter distribution was represented by a "physics function", which described the distribution expected in the absence of detector resolution effects. This was parametrised as a function of the b-baryon lifetime and was then convoluted with a "resolution function" to represent the beamspot size and the effects of the detector. The contribution not from b-baryon $\to \Lambda\mu X$ decays was described by a "background function" parametrising the behaviour of $b \to \mu$, $b \to c \to \mu$, $c \to \mu$, and fake lepton and Λ events. The relative proportions of these backgrounds were taken from the simulation, with only the mean b hadron lifetime and the impact parameter distribution of the fake leptons being fitted to the data, as described below. This background contribution was also convoluted with the resolution function. The sum of all expected contributions was then fitted to the data using a maximum likelihood technique to determine the b-baryon lifetime. The estimation of each of these components is described briefly below; full details of this analysis can be found in [22].

The physics function was determined from the simulation, using a dedicated b-baryon sample of 12000 events and by applying the same kinematical cuts as in the data. The distribution was parametrised by four exponentials, two for either sign of the impact parameter distribution. The simulation was reweighted to mimic several different b-baryon lifetimes and the variation of the seven parameters of the exponentials (three relative normalisations and four means) was determined. The uncertainty on the parameters due to the finite simulation statistics was taken as a source of systematic error, giving a contribution of 0.02 ps. The variation of the parameters with the b-baryon polarisation was

also calculated, again using a weighting technique to mimic different polarisation values. The uncertainty of the exponential parameters due to the uncertainty in the polarisation was considered as a separate source of systematic error, see Table 3.

The resolution function was determined directly from the data using a sample dominated by tracks from the primary vertex, where the width of the impact parameter distribution is due mainly to resolution effects. The above cuts were applied except that all muon identification requirements were removed, which reduced the b and c quark fractions in the sample. To further reduce these fractions, the b-tagging variable defined in [10], P_H, based on impact parameters, was calculated using the tracks in the hemisphere opposite to the b-baryon candidate. The construction of P_H was tuned [23] for both data and simulation to have a flat distribution over the range $0 < P_H < 1$ if all the tracks considered came from a single vertex, and to be shifted to lower values if they did not. To select events for the resolution function determination, P_H was required to satisfy $-log_{10}P_H < 0.5$ (i.e. $P_H > 0.316$), preferentially removing b and c quark events. It was estimated from the simulation that, in the resulting track sample, only 8% of tracks originated from decays of particles with non-zero lifetimes. The distribution of impact parameters divided by their errors for this sample was fitted using two Gaussian functions over various impact parameter ranges between ± 0.02 cm and ± 0.10 cm. The narrower of the two Gaussian functions described between 91% and 97% of the tracks and had a width, k_1, in all cases equal to one within a few percent. The wider Gaussian described a combination of the tail in the detector resolution distribution and the remaining non-zero lifetime component of the tracks; its width, k_2, varied between 2.5 and 4.0. The widths k_1 and k_2 were used to scale the impact parameter errors from their nominal values in the likelihood function described below. The variation in the fit parameters with the fitted range was taken to reflect the uncertainty in the proportions of these two components. The systematic error associated to the parametrisation of the resolution function was 0.03 ps.

The background distribution was due to two main sources: the flying and non-flying backgrounds, as in the previous analysis. The biggest contribution, $F_{fb} = 81\%$, was due to muons from b and c hadron decays. These result from decays of particles with non-zero lifetimes and their expected impact parameter distribution was parametrised directly from the simulation, again using four-fold exponential distributions as for the physics function described above. In this case, the parametrisation was done as a function of the mean b hadron lifetime, with the c hadron lifetimes fixed. The lifetime to be used for this component of the background function was estimated from the data by removing all Λ selection requirements from the right sign sample. This method was used, rather than fitting the wrong sign sample as in the previous analysis, because it provides a much larger sample (it could not be used in the previous analysis as the Λ was needed to form the vertex). The muon sample was then reasonably insensitive to the b-baryon lifetime as it was dominated by B meson decays – less than 10% of the muons were expected to originate from b-baryons. The background function was convoluted with the resolution function and
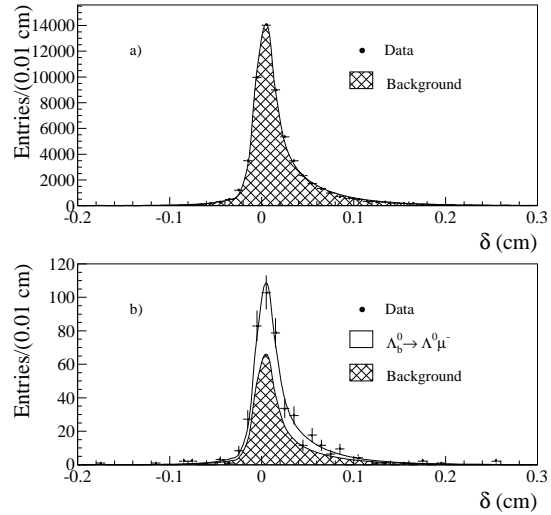

Fig. 6. Lifetime-signed impact parameter distribution for **a)** all selected muon candidates and **b)** those with an associated Λ. Also shown are the results of the fits, as described in the text, to determine the background and b-baryon lifetimes respectively

used in the maximum likelihood fit (see below) with the signal fraction, F_s, set to zero, to determine the mean b hadron lifetime of the background. The resulting value was $1.639 \pm 0.013 \, ^{+0.06}_{-0.04}$ ps; the distribution and fit are shown in Fig. 6a. The systematic error on the background lifetime is dominated by the uncertainty in the proportion of b-baryons with a fake Λ remaining in the background sample when the Λ selection requirement is reimposed; the error quoted corresponds to the full possible range of $(0 - 10)\%$.

The remaining 19% of the background was from hadrons misidentified as muons, some of which originated from particles with significant lifetimes. The impact parameter distribution of this sample was measured from the data by removing the muon identification requirements, as for the resolution function study, but without imposing the opposite hemisphere P_H cut. The resulting sample was found to have a mean impact parameter of $52\mu m$, reflecting its lifetime component, and this sample was also parametrised by a four-fold exponential, as for the physics function.

A maximum likelihood fit was performed to the 441 right sign events within the mass window specified above. The function to be maximised was the sum of the above contributions all convoluted with the resolution function:

$$L = \Sigma_i \ln[f(\delta_i, \sigma_i, \tau, \tau_{bck})],$$

with

$$f(\delta_i, \sigma_i, \tau, \tau_{bck}) = [F_s \cdot E_4(\tau) + (1 - F_s) \cdot (F_{fb} \cdot E'_4(\tau_{bck})$$

$$+(1 - F_{fb}) \cdot E''_4)] \otimes \ [(1 - \gamma) \cdot G(k_1\sigma_i) + \gamma \cdot G(k_2\sigma_i)]$$

where τ is the b-baryon lifetime, E_4 is the four-fold exponential for the muons from b-baryons, E'_4 is the one for muons from b and c background processes and E''_4 is for fake muons from misidentified hadrons. The scaling factors $k_{1,2}$ describe the narrow and wide components respectively of the resolution function, while γ is the fraction in the wide Gaussian. The proportions of the physics and flying background functions, F_s and F_{fb}, were fixed and the b hadron

Table 3. Contributions to the systematic error on the average b-baryon lifetime measured using muon impact parameters

Error source	Range of Variation	Syst. error (ps)
Signal Fraction F_s	0.38 ± 0.07	$+0.04$ -0.03
Physics Function	see text	± 0.02
Background Lifetime	$1.64 ^{+0.06}_{-0.04}$ ps	$+0.04$ -0.05
Resolution Function	see text	± 0.03
$< E_{\Lambda_b} >$ and M_{bar}	see Table 2	± 0.02
Λ_b polarisation	-0.47 ± 0.47	± 0.05
$\mathrm{Br}(\Lambda_b \to \Lambda_c \ell \nu \mathrm{n}\pi)/\mathrm{Br}(\Lambda_b \to \Lambda_c \ell \nu)$	$0 \to 0.3$	-0.03
Total systematic error	—	$+0.09$ -0.09

lifetime in the background function, τ_{bck}, was set to the value deduced from the background fit described above. The only remaining parameter was the b-baryon lifetime; the resulting value was:

$$\tau(b\text{-baryon}) = 1.10 ^{+0.19}_{-0.17} \text{ ps}$$

where the error reflects the statistical contribution only. The distribution of impact parameters and the result of the fit are shown in Fig. 6b.

The different contributions to the systematic uncertainty are listed in Table 3. The first reflects the uncertainty in the signal purity, which was estimated from the fits to the right sign and wrong sign Λ mass peaks described above. The second error arises from the finite simulation statistics used to parametrise the physics function. The next two errors are from the background and resolution function uncertainties. The main contribution to the background uncertainty was due to the effective background lifetime, in particular its systematic uncertainty. The uncertainty in the resolution function was estimated by varying the function fit range between ± 0.02 cm and ± 0.10 cm, as described above. The remaining systematic errors listed in the table result from uncertainties in the description of the b-baryon properties, as considered in the previous analysis (see Table 2). Summing the systematic uncertainties listed in Table 3 in quadrature gives an overall systematic uncertainty of ± 0.09 ps.

6 Lifetime measurement using $\Lambda_c \ell$ pairs

The third analysis presented in this paper used fully reconstructed $\Lambda_c \to pK\pi$, $\Lambda_c \to K^0 p$ and $\Lambda_c \to \Lambda 3\pi$ decays correlated with an ℓ^-. Possible sources of $\Lambda_c \ell^-$ in the same jet were:
- b-baryon semileptonic decays
- B meson semileptonic decays
- accidental correlations of a Λ_c candidate with a lepton or a fake lepton.

The $\Lambda_c \ell$ combinations from Λ_b decays were characterised by higher invariant mass and by higher transverse and longitudinal momentum of the lepton than the background pairs from other sources.

6.1 Selection of $\Lambda_c \to pK\pi$ decays

Λ_c candidates were selected by requiring:
- the proton momentum to be greater than the pion momentum,
- the total momentum to be at least 10 GeV/c,
- the angle between the total momentum of the Λ_c candidate and the flight direction, defined as the line from the primary vertex to the Λ_c vertex, to be below $90°$,
- the proton and the kaon to be tagged by the RICH.
If the RICH information was not available, the dE/dx measurement in the TPC for the proton candidate was required to be not more than 1 standard deviation above the expectation for a proton and the dE/dx measurement for the kaon candidate was required to be within 2 standard deviations of the value expected for a kaon.

6.2 Selection of $\Lambda_c \to pK^0$ decays

In the reconstruction of this decay mode, the K^0 candidates shown in Fig. 1b with invariant mass $0.480 < M(\pi\pi) < 0.515$ GeV/c^2 were used. The candidate proton track had to be uniquely identified by the RICH (i.e. the kaon hypothesis had to be excluded by the identification algorithm). To reduce the combinatorial background further, the proton track and the lepton track accompanying the K^0 candidate had to have at least two hits in the vertex detector and to fit a common decay vertex and decay length, measured from the reconstructed primary vertex, had to be "positive": i.e. the scalar product of the flight direction and the total momentum p_{tot} of the pK^0-lepton system had to be positive. Also, the projected angle in the plane transverse to the beam direction between the flight direction and p_{tot} had to be below $10°$.

6.3 Selection of $\Lambda_c \to \Lambda 3\pi$ decays

The Λ candidates shown in Fig. 1a with invariant mass $1.105 < M(p\pi) < 1.125$ GeV/c^2 were used in the reconstruction of this Λ_c decay mode. Three-prong decay vertices were fitted using tracks with total electric charge equal to the proton charge in the Λ candidate. Again the vertex had to have positive decay length and the angle between the flight direction and the total momentum of the Λ_c candidate had to be less than $10°$.

6.4 Λ_c-lepton selection and lifetime determination

The Λ_c candidates were paired with identified leptons of momentum over 3 GeV/c, within a cone of $45°$ around the Λ_c direction. The lepton had to have a transverse momentum with respect to the jet axis, again computed including the lepton itself, greater than 0.6 GeV/c. The total momentum of the lepton and the Λ_c had to exceed 18 GeV/c and the invariant mass of the $\Lambda_c \mu$ ($\Lambda_c e$) pair was required to be greater than 3.5 GeV/c^2 (3.2 GeV/c^2).

The mass plots for the Λ_c candidates are shown in Figs. 7a-c for the three channels considered. The full line (dashed line) histograms are the right sign (wrong sign) entries. The three channels are shown combined in Fig. 7d.

The b-baryon candidate vertices were reconstructed using the trajectories of the Λ_c and the lepton to fit a common vertex. In the $\Lambda_c \to pK^0$ case, the p-lepton vertex defined in the Λ_c selection was used as b-baryon candidate vertex.
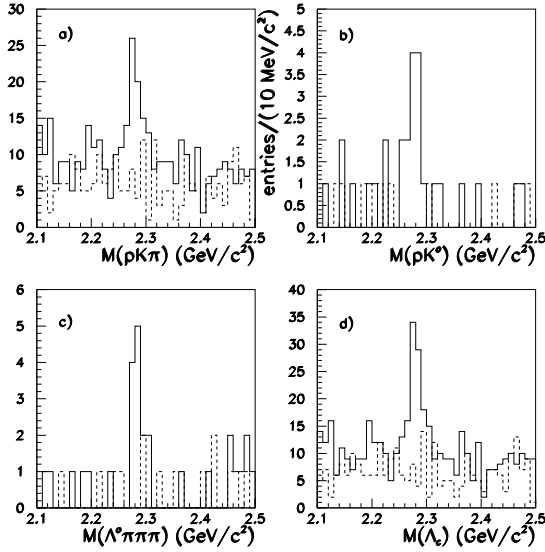
Fig. 7. Invariant mass distributions for right sign (full line) and wrong sign (dashed line) Λ_c candidates correlated with a high p_T lepton: **a)** $pK\pi$ channel, **b)** pK^0 channel, **c)** $\Lambda 3\pi$ channel, **d)** all channels combined

Fig. 8. Reconstructed Λ_c invariant mass distribution for Λ_c vertex candidates correlated with a high p_T lepton of **a)** right sign and **c)** wrong sign; **b)** lifetime distribution for b-baryon candidates, 125 right sign $\Lambda_c\ell$ vertices with $2.250 < M(\Lambda_c) < 2.310$ GeV/c^2 (shaded area in the right sign mass plot). The full lines show the fit described in the text, the dashed line is the estimated b-baryon contribution, the dotted and dot-dashed lines are the flying and non-flying backgrounds determined from **d)** the lifetime distribution of the 139 $\Lambda_c\ell$ vertices in the background sample taken from the regions in **a)** and **c)** marked by the arrows.

The b-baryon momentum was estimated with the residual energy technique:

$$E_{\Lambda_b} = E_{beam} - E_{res} = E_{beam} - E_{vis} + E_{\Lambda_c} + E_\ell$$

with the quantities defined as in Sect. 5.1. In this case the simulation showed that, due to detector inefficiencies, the b-baryon energy estimate had to be scaled by the factor 0.950 ± 0.015, where the quoted error was due to the finite simulation statistics available. This error was included in the systematic errors. If one or two additional pions were produced in the b-baryon decay, the b-baryon energy was on average respectively 3.5 or 6 GeV too low. But as the selection efficiency was lower for the multiple pion modes than for the mode with no additional pions, the effect of this uncertainty on the momentum resolution was found to be small.

A sample of 125 signal vertices was selected using right sign pairs with $2.250 < M(\Lambda_c) < 2.310$ GeV/c^2. In a similar way, a background sample of 139 vertices was defined using wrong sign pairs with $2.220 < M(\Lambda_c) < 2.340$ GeV/c^2 and "sideband" right sign pairs with $2.220 < M(\Lambda_c) < 2.250$ GeV/c^2 or $2.310 < M(\Lambda_c) < 2.340$ GeV/c^2. The resulting proper time distributions, shown in Figs. 8b and 8d, were fitted with the same technique as that used for the study of the $\Lambda\ell$ channel. In the likelihood function, the signal fraction F_s was a function of the reconstructed Λ_c invariant mass and of the decay channel, obtained from the plots shown in Figs. 7a-c. Its average value over the whole signal sample was $(69 \pm 10)\%$. The result was:

$$\tau(b - \text{baryon}) = 1.19^{+0.21}_{-0.18} \text{ ps}$$

where the error reflects the statistical contribution only. The fit gave a flying background lifetime of $1.72^{+0.16}_{-0.14}$ ps and a correlation coefficient with the b-baryon lifetime of -0.19.

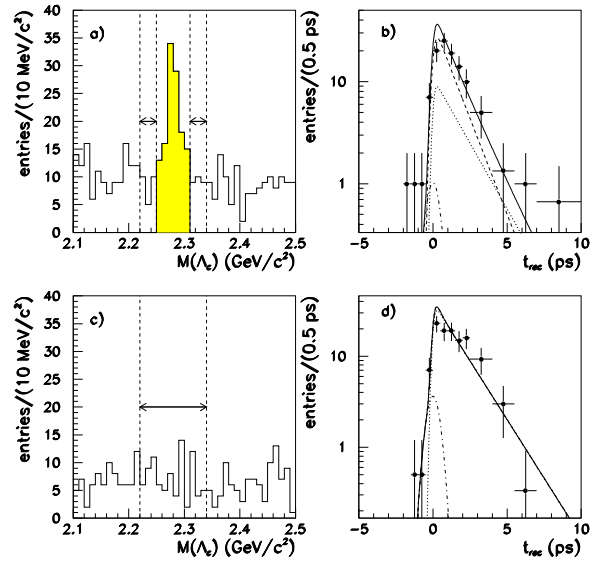The different contributions to the systematic error are shown in Table 4. The first came from the uncertainty on the

Table 4. Contributions to the systematic error on the average b-baryon lifetime measured using $\Lambda_c\ell$ correlations.

Error source	Range of Variation	Syst. error (ps)
Signal Fraction F_s	0.69 ± 0.10	± 0.02
σ_i Parametrisation	see text	± 0.04
Fit procedure bias	see text	± 0.05
$< E_{\Lambda_b} >$ and M_{bar}	see Table 2	± 0.01
$\eta(\omega) = \exp[a_{IW}(1 - \omega)]$	$a_{IW} = 1.7^{+3.3}_{-1.7}$	± 0.01
$\text{Br}(\Lambda_b \to \Lambda_c\ell\nu n\pi)/\text{Br}(\Lambda_b \to \Lambda_c\ell\nu)$	$0 \to 0.3$	-0.04
Total systematic error	—	$^{+0.07}_{-0.08}$

signal purity, which was varied in the fit within its statistical error. The σ_i parametrisation was studied in the simulation, following the procedure discussed in Sect. 5.1, and a total systematic error of 0.04 ps was assigned. The error scaling factor was 1.3 in this case. A fit to about 400 reconstructed b-baryon decays from a dedicated simulation sample of 20000 $\Lambda_b \to \Lambda_c\ell\nu(\Lambda_c \to pK\pi)$ decays gave $\tau(b\text{-baryon})= 1.26 \pm 0.05$ ps. The statistical error of this result was considered to be a systematic error from the possible bias introduced by the fitting procedure. The determination of the other entries of Table 4 also followed the discussion in Sect. 5.1 closely. The effect of the Λ_b polarisation was studied in the simulation and found to be negligible.

Summing the systematic uncertainties in quadrature gave an overall systematic uncertainty of $^{+0.07}_{-0.08}$ ps.

7 Conclusions

The average lifetime of the b-baryon was studied using two different decay channels, relying on the detection of a fast Λ or a Λ_c in the same jet as a high p_T lepton. The following results were obtained:

$$\tau(b\text{-baryon}) = (1.46^{+0.22+0.07}_{-0.21-0.09})\,\text{ps}\,(206\,\Lambda\ell\pi\text{ decay vertices}),$$

$$\tau(b\text{-baryon}) = (1.10^{+0.19+0.09}_{-0.17-0.09})\,\text{ps}\,(441\,\Lambda\mu\text{ pairs}),$$

$$\tau(b\text{-baryon}) = (1.19^{+0.21+0.07}_{-0.18-0.08})\,\text{ps}\,(125\,\Lambda_c\ell\text{ decay vertices}).$$

The statistical correlation between the first two analyses (20% of the $\Lambda\mu$ pairs used in the impact parameter measurement were already used in the $\Lambda\mu\pi$ vertex measurement) and between the Λl and $\Lambda_c l$ lepton samples (5%) was taken into account when averaging the results. The full correlation of the entries in the lower halves of Tables 2, 3 and 4 was also taken into account in combining the systematic errors. The combined result was:

$$\tau(b\text{-baryon}) = (1.254^{+0.121}_{-0.109}(stat) \pm 0.04(syst)^{+0.03}_{-0.05}(syst))\text{ps}.$$

The first systematic error resulted from the uncorrelated part of the systematic errors of the individual measurements, mainly due to experimental uncertainties. The second systematic error was due to the common uncertainty from the modelling of the b-baryon production and semi-leptonic decay.

Another measurement of the b-baryon lifetime was recently published by DELPHI [8], based on the proper decay time distribution of candidate vertices with a high momentum proton and a high p_T muon:

$$\tau(b - \text{baryon}) = (1.27^{+0.35+0.09}_{-0.29-0.09})\text{ ps}.$$

The overlap between this sample and those used in the present work is negligible. Only a small fraction (0.02 ps) of the systematic error is correlated with the errors of the analyses reported in this paper. Combining this measurement with those presented here gives:

$$\tau(b - \text{baryon}) = (1.255^{+0.115}_{-0.102} \pm 0.05)\text{ ps}.$$

This result for the average b-baryon lifetime includes and therefore supersedes all previous Delphi measurements [4, 8].

It should be stressed that all these results correspond to means of the lifetimes of all b-baryons, weighted by their production rates in b-jets at LEP and their semileptonic branching ratios into the channels considered. The result based on $\Lambda_c\ell$ decay vertices, namely $\tau(b\text{-baryon}) = (1.19^{+0.21+0.07}_{-0.18-0.08})$ ps, might be considered as the one most representative of the lifetime of the Λ_b baryon. However, the observed production rate of the Ξ_b [19], which is the other weakly decaying b-baryon expected to be most abundantly produced in b-jets, is such that all samples are expected to be dominated by Λ_b baryons.

References

1. UA1 Collaboration, C. Albajar et al., Phys. Lett. **B273** (1991) 540.
2. R422 collab., G. Bari et al., Nuovo Cimento **104A** (1991) 1787.
3. ALEPH Collaboration, D. Decamp et al., Phys. Lett. **B278** (1992) 209; OPAL Collaboration, P. D. Acton et al., Phys. Lett. **B281** (1992) 394.
4. DELPHI Collaboration, P. Abreu et al., Phys. Lett. **B311** (1993) 379.
5. ALEPH Collaboration, D. Buskulic et al., Phys. Lett. **B297** (1992) 449; OPAL Collaboration, R. Akers et al., Phys. Lett. **B316** (1993) 435.
6. I.I. Bigi and N.G. Uraltsev, Phys. Lett. **B280** (1992) 271; I.I. Bigi, 'Lifetimes of Heavy Flavour Hadrons', UND-HEP-95-BIG06, Invited Lecture at the 6th Int. Symp. on Heavy Flavour Physics, Pisa, Italy, June 1995.
7. ALEPH Collaboration, D. Buskulic et al., Phys. Lett. **B357** (1995) 685; OPAL Collaboration, R. Akers et al., Phys. Lett. **B353** (1995) 402 OPAL Collaboration, R. Akers et al., Z. Phys. **C69** (1996) 195.
8. DELPHI Collaboration, P. Abreu et al., Z. Phys. **C68** (1995) 375.
9. DELPHI Collaboration, P. Aarnio et al., Nucl. Instr. Meth. **A303** (1991) 233.
10. DELPHI Collaboration, P. Abreu et al., 'Performance of the DELPHI Detector', CERN-PPE/95-194, to be published in Nucl. Instr. Meth. **A**.
11. V. Chabaud et al., Nucl. Instr. Meth. **A368** (1996) 314.
12. E.G. Anassontzis et al., Nucl. Instr. Meth. **A323** (1992) 351.
13. DELPHI Collaboration, P. Abreu et al., Nucl. Phys. **B418** (1994) 403.
14. W. Adam et al., DELPHI RICH collab., Proceedings of the 1995 Int. Workshop on Ring Imaging Cherenkov Detectors, Uppsala 1995, to be published in Nucl. Instr. Meth. **A**.
15. T. Sjostrand, Comp. Phys. Comm. **82** (1994) 74.
16. T. Sjostrand et al., Comp. Phys. Comm. **39** (1986) 347; **43** (1987) 367.
17. Particle Data Group, Phys. Rev. **D50** (1994) 1173.
18. V. Gibson, Proc. of XXVII International Conference on High Energy Physics, eds. P.J. Bussey and I.G. Knowles, IOP (1994), 507.
19. DELPHI Collaboration, P.Abreu et al., 'Measurement of the production of Ξl pairs in jets at LEP and interpretation of their origin in terms of strange-beauty baryon decays', contributed paper gls0166 to ICHEP94, the 27th Int. Conf. on High Energy Physics, Glasgow 1994. P. Abreu et al., Z. Phys. **C68** (1995) 541.
20. N. Isgur and M.B. Wise, Phys. Lett. **B232** (1989) 113; N. Isgur and M.B. Wise, Phys. Lett. **B237** (1990) 527.
21. LEP B lifetimes Working Group, 'Averaging lifetimes for B hadron species at LEP', DELPHI 94-164 Phys 467 (1994).
22. S. Bosworth, 'A Measurement of the B-Baryon Lifetime', D.Phil. Thesis, University of Oxford, 1995.
23. G.V. Borisov and C. Mariotti, 'Fine Tuning of the Impact Parameter Resolution in the DELPHI Detector', to be published in Nucl. Instr. Meth. **A**.